

Peptide Variants of Viral CTL Epitopes Mediate Positive Selection and Emigration of Ag-Specific Thymocytes In Vivo¹

Masha Fridkis-Hareli,*[†] Pedro A. Reche,*[†] and Ellis L. Reinherz^{2*}[†]

During development, thymocytes carrying TCRs mediating low-affinity interactions with MHC-bound self-peptides are positively selected for export into the mature peripheral T lymphocyte pool. Thus, exogenous administration of certain altered peptide ligands (APL) with reduced TCR affinity relative to cognate Ags may provide a tool to elicit maturation of desired TCR specificities. To test this "thymic vaccination" concept, we designed APL of the viral CTL epitopes gp33–41 and vesicular stomatitis virus nucleoprotein octapeptide N52–59 relevant for the lymphocytic choriomeningitis virus-specific P14- and vesicular stomatitis virus-specific N15-TCRs, respectively, and examined their effects on thymocytes in vivo using irradiation chimeras. Injection of APL into irradiated congenic (Ly-5.1) mice, reconstituted with T cell progenitors from the bone marrow of P14 RAG2^{-/-} (Ly-5.2) or N15 RAG2^{-/-} (Ly-5.2) transgenic mice, resulted in positive selection of T cells expressing the relevant specificity. Moreover, the variants led to export of virus-specific T cells to lymph nodes, but without inducing T cell proliferation. These findings show that the mature T cell repertoire can be altered by in vivo peptide administration through manipulation of thymic selection. *The Journal of Immunology*, 2004, 173: 1140–1150.

Naive T cells expressing a highly diverse TCR repertoire are generated in the thymus from bone marrow (BM)³ lymphoid precursors (reviewed in Ref. 1). Upon entering the thymus, T cell progenitors proliferate and undergo a complex series of gene rearrangement events leading to cell surface TCR expression and subsequent differentiation (reviewed in Refs. 2 and 3). It has been demonstrated that peptides bound to the MHC molecules within the thymus control both positive and negative selection (reviewed in Ref. 4). During selection of the TCR repertoire, thymocytes that carry TCRs having low-affinity interactions with MHC-bound self-peptides are positively selected, and are exported into the pool of mature peripheral lymphocytes. In contrast, thymocytes bearing those TCRs that recognize self-peptides with high affinity are eliminated (3).

Single amino acid substitutions in either the MHC or the peptide dramatically alter recognition by T cells (5, 6). Analysis of crystal structures of $\alpha\beta$ TCR/class I MHC complexes have demonstrated that peptide specificity of T cells is primarily determined by the interaction between the CDR of the TCR-V α and -V β domains and the peptide side chains, which protrude of the peptide-binding groove of MHC molecules toward the two TCR-CDR3 loops. Structural studies of peptide/MHC complexes (pMHC) have provided detailed information about the conformation of peptide when

bound to MHC molecules (reviewed in Refs. 7 and 8). The peptide-binding groove of MHC molecules is composed of two helices on top of an eight-strand anti-parallel β -pleated sheet. The peptide-binding groove contains various binding pockets, the shape and charge of which are dependent on the highly polymorphic amino acids characteristic of a given MHC allele, which in turn selectively determines the spectrum of peptides that may bind to it (reviewed in Ref. 9 and references therein).

Much of the recent work on thymic selection was influenced by experiments that examined T cell responses to peptide analogues derived from the antigenic peptide by substitution of amino acid residues involved in interactions with the TCR. Such peptide analogues, so-called altered peptide ligands (APL), can generate qualitatively different T cell responses compared with those produced by the antigenic peptide (10). In particular, some APL were shown to act as TCR antagonists and inhibit T cell responses to the antigenic peptide (11). Several studies have shown that antagonist peptides are capable of positively selecting (12, 13), negatively selecting (14), or otherwise altering (15) selection of thymocytes.

Thymic selection processes have also been addressed in structural terms using TCR-transgenic mice. For example, in N15 transgenic mice carrying a TCR specific for the vesicular stomatitis virus nucleoprotein octapeptide N52–59 (VSV8) in the context of H-2K^b, a weak agonist peptide variant inducing positive selection has been identified (16). This variant is identical with the VSV8 peptide except for substitution of leucine for valine at the P4 peptide residue (L4). The cognate viral peptide ligand, VSV8, triggers negative selection. Another TCR transgenic mouse model, P14, expressing a TCR specific for the D^b-restricted immunodominant lymphocytic choriomeningitis virus epitope gp33–41 has been developed (17). This system has been widely used to study the effect on thymocyte development of mutations in gp33–41 peptides that interact either with the binding pockets of D^b (18) or with the TCR contact residues, using fetal thymic organ culture (FTOC; reviewed in Ref. 19). The crystal structure of gp33/H-2D^b shows that conserved single mutations at positions 4 or 6 of the peptide are solvent exposed and presumably function as TCR contacts (20, 21). In yet a third TCR transgenic mouse model, F5, where the TCR recognizes a nucleoprotein peptide of the influenza virus

*Laboratory of Immunobiology, Department of Medical Oncology, Dana-Farber Cancer Institute, Boston, MA 02115; and [†]Department of Medicine, Harvard Medical School, Boston, MA 02115

Received for publication January 22, 2004. Accepted for publication May 3, 2004.

The costs of publication of this article were defrayed in part by the payment of page charges. This article must therefore be hereby marked *advertisement* in accordance with 18 U.S.C. Section 1734 solely to indicate this fact.

¹ This work was supported by National Institutes of Health Grant AI50900 and the Molecular Immunology Foundation

² Address correspondence and reprint requests to Dr. Ellis L. Reinherz, Dana-Farber Cancer Institute, 44 Binney Street, Boston, MA 02115. E-mail address: ellis_reinherz@dfci.harvard.edu

³ Abbreviations used in this paper: BM, bone marrow; pMHC, peptide/MHC complex; APL, altered peptide ligand; VSV8, vesicular stomatitis virus nucleoprotein octapeptide N52–59; FTOC, fetal thymic organ culture; DP, double positive; DN, double negative; SP, single positive; RTE, recent thymic emigrant; AICD, activation-induced cell death.

NP366–379 in the context of H-2D^b (22, 23), the peptide antagonist mediated positive selection in FTOC (23, 24), whereas the cognate peptide itself led to deletion of CD4⁺CD8⁺ (double-positive (DP)) thymocytes (25).

Variants of peptides derived from infectious agents or tumor Ags could, in principle, mediate positive selection and export of specific T cells from the thymus. As such, these APL might be candidates for manipulating the thymic repertoire *in vivo*, controlling the generation of naive and memory T cells within the peripheral lymphoid compartment. This “thymic vaccination approach” would aim to deliver, by parenteral administration, positively selecting APL of cognate Ags to elicit maturation of thymocytes with desired TCR specificities at the level of thymic repertoire development. Expanding repertoire generation has enormous potential in aiding the organism’s fight against infections or in affording tumor immunity. To test this concept, we have designed variants of gp33–41 and VSV8 peptides with substitutions at the amino acid residues interacting with the TCR and examined their effects on thymocyte maturation and emigration *in vivo* in two well-defined systems.

Materials and Methods

Mice

N15 tg^{+/+} RAG2^{-/-} H-2^b mice were generated as described previously (26). P14 tg^{+/+} RAG2^{-/-} H-2^b transgenic mice were obtained from Tac-onic Farms (Germantown, NY). Congenic strains C57BL/6 (Ly-5.2) and C57BL/6 (Ly-5.1) were obtained from The Jackson Laboratory (Bar Harbor, ME). Mice were sex matched and used at 3–4 wk of age for peptide injections and at 7–11 wk of age for other manipulations. Mice were maintained and bred under sterile barrier conditions at the animal facility of the Dana-Farber Cancer Institute (Boston, MA).

Peptide synthesis

The peptide gp33–41 (KAVYNFATC) and its variants, Y4S/F6A (KAVS NAATC) and A7E (KAVYNFETC), were synthesized by standard solid phase methods with the modification of C to M (C9M) to prevent dimer formation mediated by free sulfhydryl-groups. N52-59 (VSV8, RGYVYQGL; Ref. 27) and its variant, L4, (RGYLYQGL) were also made and all peptides purified by reverse phase HPLC (Hewlett Packard HPLC 1100; Hewlett Packard, Palo Alto, CA).

Abs and flow cytometric analysis

All anti-mouse mAbs were purchased from BD Pharmingen (San Diego, CA). For flow cytometry, single cell thymocyte, splenocyte, or lymph node suspensions were prepared in PBS containing 2% FCS and 0.05% NaN₃. Cells were stained at 1 × 10⁶ cells per 100 μl in PBS (2% FCS and 0.05% NaN₃) containing the Abs at saturating concentrations. Phenotypes and proportions of cell subsets were analyzed by three-color flow cytometry using a FACScan (BD Biosciences, San Jose, CA) and the CellQuest program (BD Biosciences). Dead cells were excluded from the analysis by forward and side scatter gating.

For sorting, BM cells or splenocytes from N15 RAG2^{-/-} and P14 RAG2^{-/-} mice were prepared as single-cell suspensions and stained at 30 × 10⁶ cells per milliliter in PBS containing the following mAbs at saturating concentrations: CyChrome-conjugated anti-CD8 and PE-conjugated anti-CD44 Abs were used to sort CD8⁺CD44⁻ splenocytes; for BM, FITC-conjugated anti-CD4, -CD8α, -CD45R/B220, -Ly-6G, and -CD11b were used to sort cells negative for the mixture of the above Abs. Cells were sorted under sterile conditions into tubes containing PBS: 2% FCS and 0.5% gentamicin using a MoFlo (DakoCytomation, Carpinteria, CA) and the Summit program (DakoCytomation).

Injection of cells and peptides

Sorted splenocytes or BM cells (1 × 10⁶ cells per 100 μl PBS/2% FCS per mouse) were transferred *i.v.* into irradiated (700 rad, split dose 450 and 250 at a 3-h interval) B6 Ly-5.1 mice several hours after irradiation (¹³⁷Cs source). Peptides (25 μg/100 μl PBS per mouse) were injected *i.v.* 4 days after the transfer of splenocytes, or 3–4 wk after the transfer of BM cells. N15-specific peptides (VSV8 and L4) were injected once, whereas P14-related peptides (gp33–41_{C9M}, Y4S/F6A_{C9M}, and A7E_{C9M}) were injected once or three times every 24 h.

Tetramer preparation and staining

Tetramers consisting of complexes of biotinylated H-2D^b refolded with the gp33–41_{C9M}, Y4S/F6A_{C9M}, or A7E_{C9M} peptides were produced using the method previously described (28). For immunofluorescence analysis, 1 × 10⁶ cells (thymocytes, splenocytes, or lymph node cells) were incubated with FITC anti-CD8α mAb for 1 h at 4°C, followed by addition of 0.5 μg of PE-labeled tetramers gp33–41_{C9M}/D^b, Y4S/F6A_{C9M}/D^b, or A7E_{C9M}/D^b and CyChrome-anti-CD4 and incubation for another hour. After two washes, cells were analyzed on a FACScan as described above.

Miscellaneous assays

Assays for RMA-S H-2D^b stabilization, apoptosis, proliferation, BrdU, CFSE, and intracellular cytokine staining were done as detailed elsewhere (29–31).

Results

Design and initial characterization of gp33–41 variant peptides

gp33–41 is the cognate peptide Ag of the P14 TCR (Vα2 and Vβ8) and triggers negative selection of P14-bearing DP thymocytes (reviewed in Ref. 19). Structural variants of gp33–41 were designed to influence the outcome of thymocyte selection by altering the affinity of the pMHC ligand interactions with the TCR. No change was made in the peptide anchor residues that occupy the binding pockets of H-2D^b, thus ensuring proper peptide presentation in the context of MHC. Indeed, the crystal structure of the gp33–41/H-2D^b complex shows that the side chains of amino acid residues at peptide positions p1, p4, p6, p7, and p8 are exposed to the solvent (20, 21). To design a variant with reduced affinity for the P14 TCR, we have introduced two types of mutations: in one mutant, both centrally disposed p4 and p6 residues have been modified (Tyr (Y) to Ser (S) at p4 and Phe (F) to Ala (A) at p6). In the other, Ala (A) was substituted with Glu (E) at p7. Both variants were synthesized in two alternative forms, one with the natural amino acid Cys (C) at the anchor residue p9, and the other with Met (M) at p9, thus avoiding any potential peptide dimerization mediated by free SH-groups. This modification was previously shown to stabilize the binding of gp33–41 peptide to H-2D^b (32). The sequence of gp33–41 and the variant peptides and the relevant gp33–41D^b structure are shown in Fig. 1A.

Next, we verified whether these gp33–41 variant peptides were able to bind to H-2D^b molecules using RMA-S cells. To this end, RMA-S cells were incubated with the peptides listed in Fig. 1A, and the extent of staining with anti-H-2D^b Abs on the surface of peptide-loaded RMA-S cells was measured by FACS. The binding profiles are shown in Fig. 1B. Variant peptides Y4S/F6A_{C9M} and A7E_{C9M} bound equally well to H-2D^b molecules, and in a similar fashion compared with the cognate gp33–41_{C9M} epitope, suggesting that amino acid substitutions at peptide residues p4, p6, and p7 indeed do not affect peptide binding, and, by extension, peptide presentation to T cells.

To evaluate the functional potential of T cells in mice injected with gp33–41 variant peptides, splenocyte, and lymph node T cell responses to the above peptides were examined for proliferation and cytokine secretion. Both splenocytes (Fig. 1C) and lymph node T cells (data not shown) proliferated *in vitro* in response to the gp33–41_{C9M} peptide, reaching a peak response at 10⁻¹⁰ M. The highest response to the A7E_{C9M} mutant peptide was achieved at the peptide concentration of 10⁻⁸ M (Fig. 1C). It should be noted that when a similar assay was performed using the gp33–41 variant peptides, the potency of either of these peptides at the peak of response was reduced by two logs relative to gp33–41_{C9M}, namely, 10⁻⁸ M for the gp33–41 and 10⁻⁶ M for the A7E mutant (data not shown). In contrast, incubation of T cells with the Y4S/F6A_{C9M} peptide resulted in essentially no response at any peptide concentration, possibly due to low affinity interactions with the

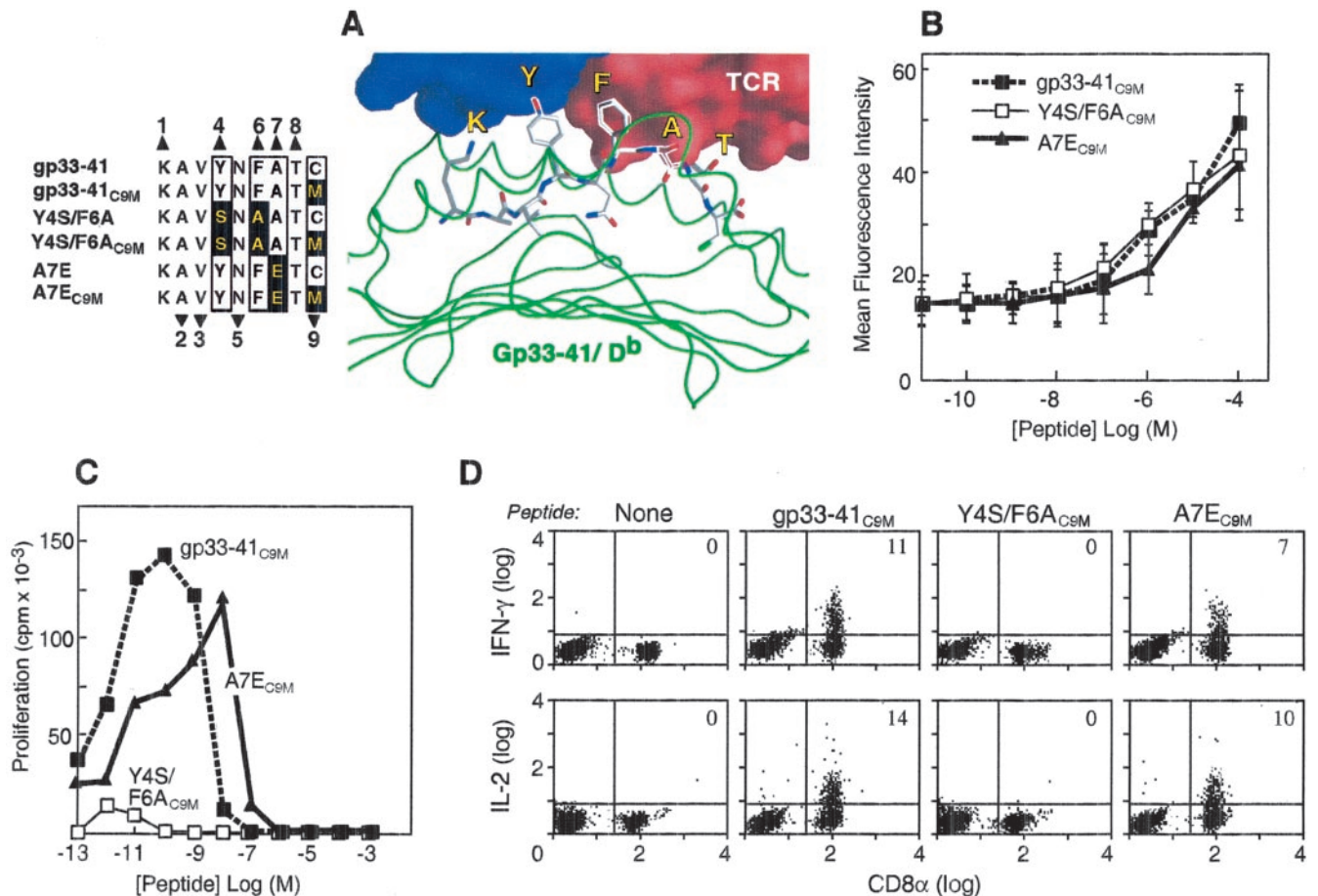


FIGURE 1. Design and initial characterization of gp33-41. *A*, Structural basis for peptide design. The figures show the three-dimensional rendition of the gp133-142 peptide in complex with the D^b molecule (worm representation; Brookhaven Protein Data Bank (PDB):1FG2) and a hypothetical TCR (surface representation). Positions of the gp133-142 peptide that can potentially interact with the TCR V domains are labeled. TCR chosen to render this figure correspond to that of the single-chain variable fragment BM3.3 TCR in complex with the Pbm1/K^b (peptide/MHC) complex (PDB:1FO0). A sequence alignment of the gp133-142 peptide and derived APLs is shown next to the worm representation of the D^b molecule. Amino acid differences are shaded in black, and peptide anchor and peptide TCR-contact residues are indicated with triangles, below and above the alignment, respectively. *B*, gp33-41_{C9M} variant peptides bind to H-2D^b molecules on RMA-S cells with similar affinities. RMA-S cells were incubated with the above peptides at the indicated concentrations, followed by immunofluorescence assay using the H-2D^b-specific mAb, HB27. Results are represented as mean \pm SD of four independent experiments. *C*, Lack of proliferation of naive P14 T cells in response to the Y4S/F6A_{C9M} variant. Splenocytes were incubated in vitro with the indicated concentrations of gp33-41_{C9M} variant peptides. Mean of triplicate cultures is shown. Results are representative of four independent experiments. *D*, Lack of IFN- γ and IL-2 production upon stimulation of naive T cells from P14 RAG2^{-/-} mice by Y4S/F6A_{C9M} variant. Splenocytes were incubated in vitro with gp33-41_{C9M} variant peptides, followed by intracellular staining protocol. Percentages of cytokine-producing SP CD8 cells were determined by flow cytometry. Results are representative of three independent experiments.

TCR. Consistent with the proliferation data, an assay for intracellular cytokine staining with anti-IFN- γ or -IL-2 Abs showed the highest levels of both cytokines when splenocytes were incubated with the gp33-41_{C9M}, slightly lower levels in the presence of A7E_{C9M} and no cytokine secretion in the presence of Y4S/F6A_{C9M} peptide (Fig. 1D). Collectively, our results suggest that the Y4S/F6A_{C9M} variant peptide (and Y4S/F6A, data not shown) does not elicit responses of mature T cells from P14 RAG2^{-/-} mice.

Effect of gp33-41 variant peptides on thymocyte development in P14 RAG2^{-/-} mice

To examine the effect of gp33-41 variant peptides on thymocyte development in P14 RAG2^{-/-} mice, we developed a protocol for peptide injection in vivo. Earlier studies using N15 RAG2^{-/-} transgenic mice showed that a single i.v. injection of VSV8 peptide leads to a severe depletion of DP thymocytes, whereas a variant of VSV8, L4 (V4L mutation at p4) mediates positive selection in FTOC (16). Here, in contrast, a single injection of gp33-41_{C9M}

peptide into P14 RAG2^{-/-} transgenic mice caused only a modest reduction in the percentage of the DP thymocytes, although the total number of thymocytes was reduced by approximately two-thirds (Fig. 2A, upper panel). Note that the down-regulation of both CD4 and CD8 on the DP thymocytes due to impending clonal deletion causes “spillover” into a single-positive (SP) CD8 gate, resulting in a higher percentage of SP CD8 cells as compared with the PBS control. However, injection of the double mutant Y4S/F6A_{C9M} led to an unexpected tripling of total cell numbers, without perturbation in subset distribution. In contrast, A7E_{C9M} had no effect on the thymocyte number and only a slight increase in the percentages of DP or SP CD8 thymocyte subsets.

To next investigate the effect of variant peptides on the expression of thymocyte surface markers characteristic of maturation and/or activation states, cells were examined by triple-color immunofluorescence using various mAbs. A representative staining profile of SP CD8 thymocytes for the expression of β_7 integrin, a marker linked to thymocyte emigration (33), is shown in Fig. 2A

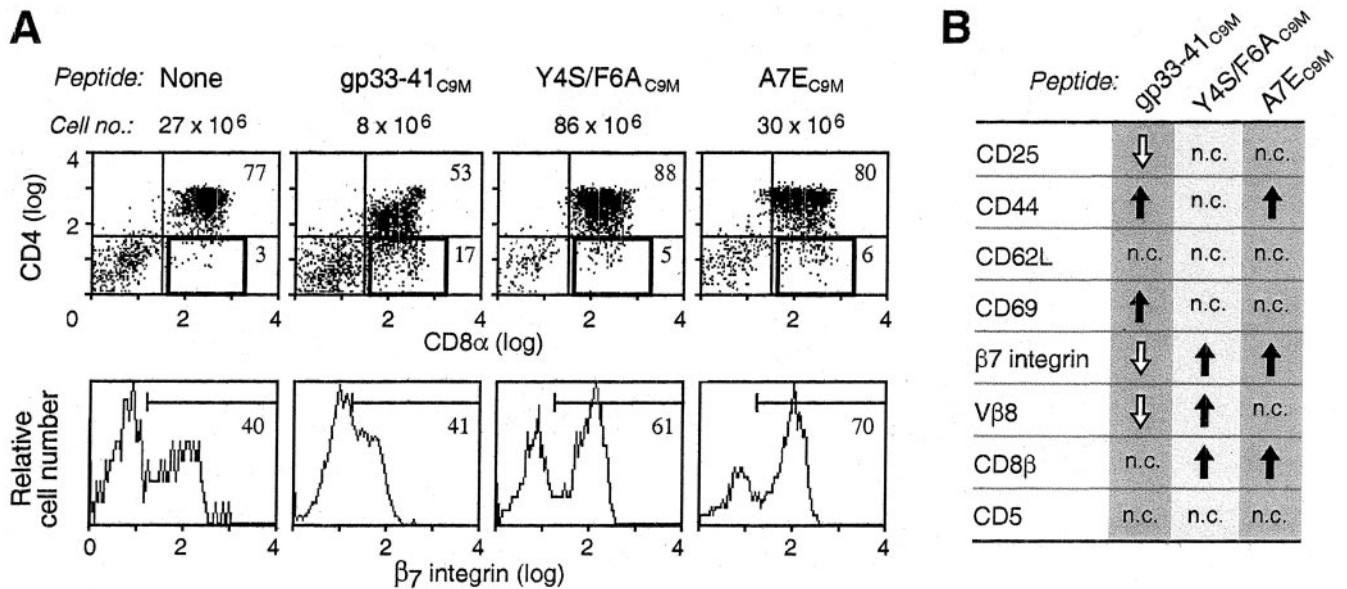


FIGURE 2. Modulation of thymocyte number and phenotype in P14 RAG2^{-/-} mice by the Y4S/F6A_{C9M} variant. **A**, Triple-staining profiles of thymocytes from mice injected with gp33-41 variants. *Upper panel*, the CD4/CD8 α profiles in thymocytes are altered in the presence of gp33-41 variant peptides. Thymocytes from P14 RAG2^{-/-} mice at 3–4 wk of age, injected with gp33-41_{C9M} variants 18 h earlier (25 μ g i.v.), were stained with CyChrome-anti-CD4, PE-anti-CD8 α FITC-anti- β_7 integrin. The percentages of DP and SP CD8 subsets after gating on 50,000 live cells are indicated. *Lower panel*, The histograms of β_7 integrin expression on the gated SP CD8 thymocytes. The numbers represent the percentages of β_7 integrin-positive cells. **B**, Expression of several T cell markers is altered on SP CD8 thymocytes from mice injected with gp33-41_{C9M} variant peptides. Thymocytes were stained with CyChrome-anti-CD4, PE-anti-CD8 α , and FITC-anti-CD25, -CD44, -CD62L, -CD69, - β_7 integrin, -V β 8, -CD8 β , and -CD5. Arrows up and down indicate up-regulation and down-regulation, respectively, as expressed by change in the MFI and/or percentage of positive cells; n.c., no change in the expression was detected as compared with control mice (injected with PBS). Results are representative of four independent experiments.

(*lower panel*). Injection with the gp33-41_{C9M} peptide led to a decrease in the β_7 integrin expression level on SP CD8 thymocytes as compared with the control PBS-injected mouse (mean fluorescence intensity (MFI) 50 vs 108, respectively), despite essentially no change in the percentage (40–41%) of anti- β_7 integrin reactive cells. Both Y4S/F6A_{C9M} and A7E_{C9M} induced an increase in the percentage of this thymocyte population (61–70%) without changing β_7 integrin levels on individual thymocytes. A complete analysis of thymocyte markers is summarized in Fig. 2B. Higher levels of CD44 and CD69 were observed on SP CD8 thymocytes injected with the gp33-41_{C9M} peptide. In contrast, Y4S/F6A_{C9M} had no effect on the above markers, but V β 8 (P14-specific TCR), β_7 integrin, and CD8 β expression were up-regulated. There was an increase in the expression of CD44, CD8 β , and β_7 integrin on SP CD8 thymocytes of mice injected with the A7E_{C9M} variant. These results indicated that a single injection of gp33-41_{C9M} and Y4S/F6A_{C9M} affected both the cell numbers and expression of thymocyte markers, suggestive of early events in thymocyte activation. A7E injection did not alter cell numbers, but affected thymocyte marker expression. Such phenotypic changes may be reflective of molecular up- or down-regulation and/or selection of cellular subpopulations. Although not shown, alterations in cellular phenotypes were evident at the earliest interval examined postinjection (6 h) as well.

While reducing absolute cell number, a single dose of gp33-41 had little influence on the percentage of DP thymocytes in P14 RAG2^{-/-} mice. Therefore, we have injected gp33-41 variants every 24 h for 3 days and found that under these conditions the DP thymocyte depletion was pronounced, leading to a nearly total elimination of these thymocytes (Fig. 3A). This observation is consistent with that made in another H-2D^b-restricted TCR transgenic system, F5, where multiple peptide injections were also required (34). In contrast, almost total elimination of N15 RAG2^{-/-} DP thymocytes was achieved by a single K^b-binding VSV8 cognate

peptide injection (Refs. 16 and 26 and data not shown). Whether this difference is a result of greater CD8 $\alpha\beta$ coreceptor binding to H-2K^b vs D^b (28), the higher copy number of peptide complexes with K^b vs D^b molecules (28), or TCR affinity differences remains to be determined. Surprisingly, injection with the Y4S/F6A_{C9M} mutant resulted in a significant increase in the total number of thymocytes as well as DP thymocyte subpopulation. In contrast, the A7E_{C9M} variant had no effect on the thymocyte counts (Fig. 3A). The expression of the examined phenotypic markers on SP CD8 thymocytes followed a similar trend after third injection (data not shown) as compared with a single peptide injection (Fig. 2B).

The possibility that the unusual increase in the number of DP thymocytes following exposure to the Y4S/F6A peptide might be due to cellular proliferation and attendant DNA synthesis was examined by BrdU incorporation assay as shown in Fig. 3B. As expected, lower BrdU incorporation was detected in each of the thymocyte subpopulations (double-negative (DN), DP, and SP CD8) of mice injected with gp33-41_{C9M}, supporting previous observations on negative selection and apoptosis by this ligand (19). More importantly, no significant difference in the amount of BrdU incorporation was found in thymocytes of mice injected with either Y4S/F6A_{C9M} or A7E_{C9M} variants, compared with the control PBS-injected mice. As a consequence, we wondered whether Y4S/F6A peptide might increase the DP subpopulation by preventing apoptosis. To test this possibility, staining of cells from mice injected with gp33-41 variants with anti-annexin V mAb was performed (Fig. 4). Indeed, there was an increase in the percentage of annexin V⁺ cells (12%) in mice injected with gp33-41_{C9M} peptide, suggestive of apoptosis. In contrast, no such phenomenon was observed upon injection of either Y4S/F6A_{C9M} or A7E_{C9M} variants; in those cases, values were comparable to the control mouse. We reasoned that if the Y4S/F6A peptide competes with apoptosis-inducing peptides for binding to H-2D^b molecules on the cell

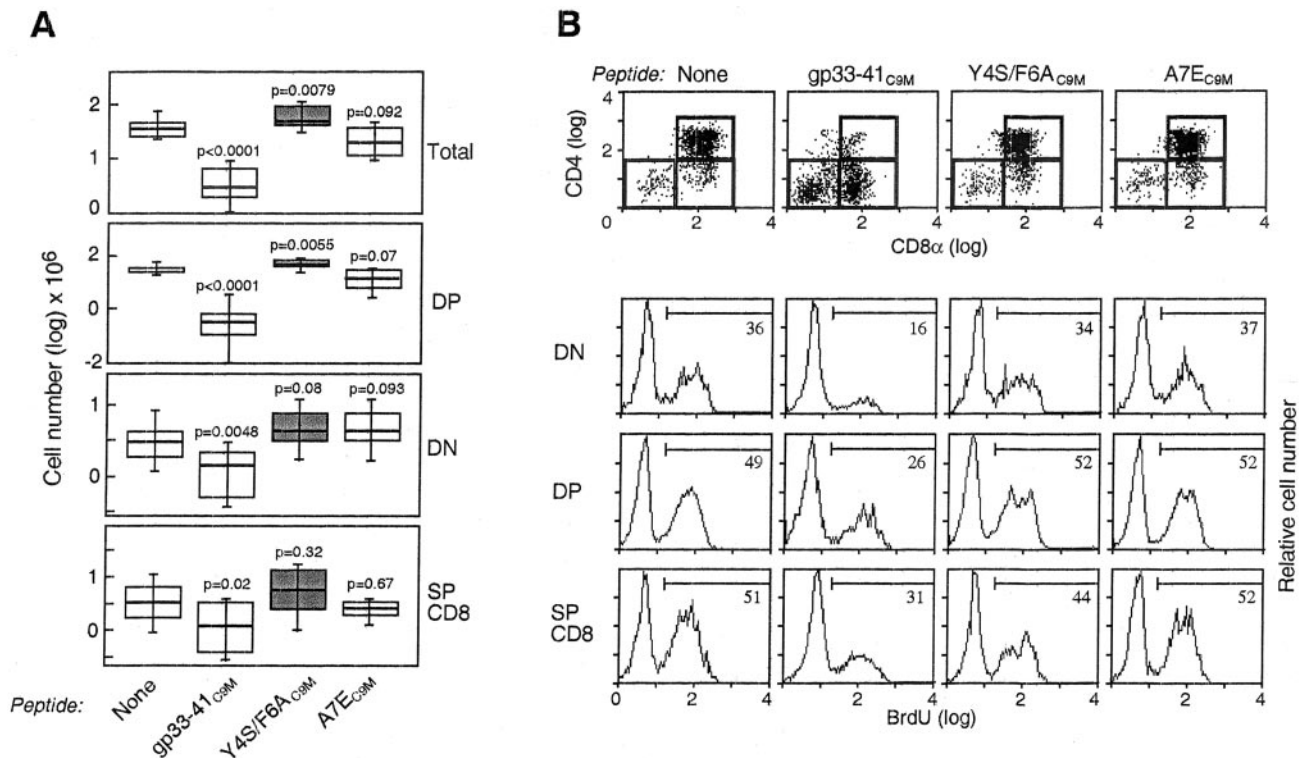


FIGURE 3. Quantitative changes in thymocyte subpopulations following multiple injections of the Y4S/F6A_{C9M} variant. **A**, Cell numbers of thymocyte subpopulations in P14 RAG2^{-/-} mice. P14 RAG2^{-/-} mice at 3–4 wk of age were injected i.v. three times every 24 h with 25 μg of each peptide and sacrificed 18 h following the third injection. Thymocytes were double-stained with CyChrome-anti-CD4 and PE-anti-CD8α, and the expression of CD4 and CD8α was detected by flow cytometry after gating on 50,000 cells. The distributions of log₁₀ cell counts × 10⁶ are shown in box plots. The box in the plot extends from the first to the third quartiles of the data; the line in the middle of the box plot denotes the median. The lines above and below the boxes extend to the largest observation (respectively, smallest observation) that is below the third quartile plus 1.5 × the interquartile range (respectively, the largest observation above the first quartile minus 1.5 × the interquartile range). Individual points shown in the graphs are >1.5 × the interquartile range from the nearest quartile. All plots were drawn in Stata version 8.0 for MS Windows (Microsoft, Redmond, WA). Data represent 10–12 independent experiments. **B**, gp33–41_{C9M} variant peptides do not alter DNA synthesis in residual thymocytes. P14 RAG2^{-/-} mice were injected three times, as indicated in **A**. On the day of the last injection, mice were given 1 mg of BrdU twice at a 4-h interval, i.p. 18 h later, and thymocytes were triple-stained with CyChrome-anti-CD4, PE-anti-CD8α, and FITC-anti-BrdU. The histograms of BrdU staining on the gated DN, DP, and SP CD8 thymocytes are shown. The numbers represent the percentages of BrdU-positive cells. Results are representative of three independent experiments.

surface, then Y4S/F6A may “rescue” thymocytes from undergoing cell death. Competitive binding assays, in which P14 RAG2^{-/-} mice were injected with the mixtures of the negatively selecting cognate peptide gp33–41_{C9M} and Y4S/F6A_{C9M} variant, were per-

formed in vivo. The results in Fig. 5 show that, as predicted, increasing the amount of Y4S/F6A peptide in the injection mixture resulted in a higher number of total and DP thymocytes. Thus, we infer that the Y4S/F6A variant may compete with other negatively

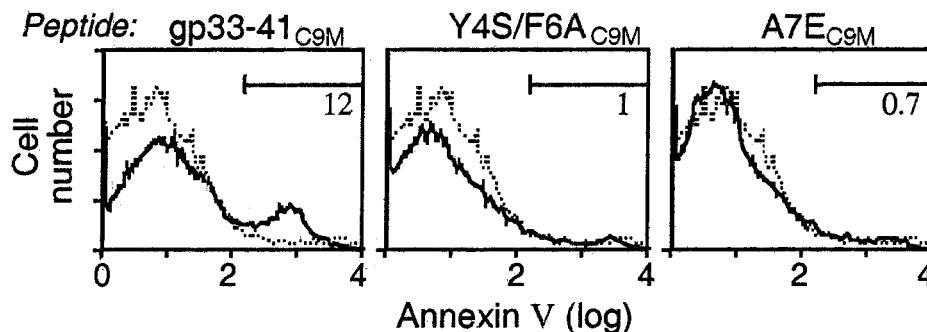


FIGURE 4. Decreased apoptotic cell death in thymocytes of P14 RAG2^{-/-} mice injected with the Y4S/F6A_{C9M} variant 6 h previously. Treatment of P14 RAG2^{-/-} mice with gp33–41_{C9M} resulted in reduction of thymocyte number (without gp33–41_{C9M}, 4.6×10^7 cells per thymus; with gp33–41_{C9M}, 3.2×10^7 cells per thymus). By contrast, P14 RAG2^{-/-} mice injected with Y4S/F6A_{C9M} variant showed increase in the number of thymocytes (7×10^7 cells per thymus), whereas injection with A7E_{C9M} variant resulted in little changes in thymocyte numbers (4×10^7 cells per thymus). Total thymocytes were stained with FITC-anti-annexin V and assayed by flow cytometry. Dead cells were gated out using propidium iodide to reveal the proportion of live thymocytes undergoing early stages of apoptosis. The histograms of annexin V staining on the propidium iodide-negative live thymocytes are shown. Histograms of PBS-injected thymocyte staining (dotted lines) were superimposed on those of peptide-treated thymocyte profiles (solid lines). The numbers represent the percentages of annexin V⁺ apoptotic thymocytes in mice injected with gp33–41_{C9M} variant peptides.

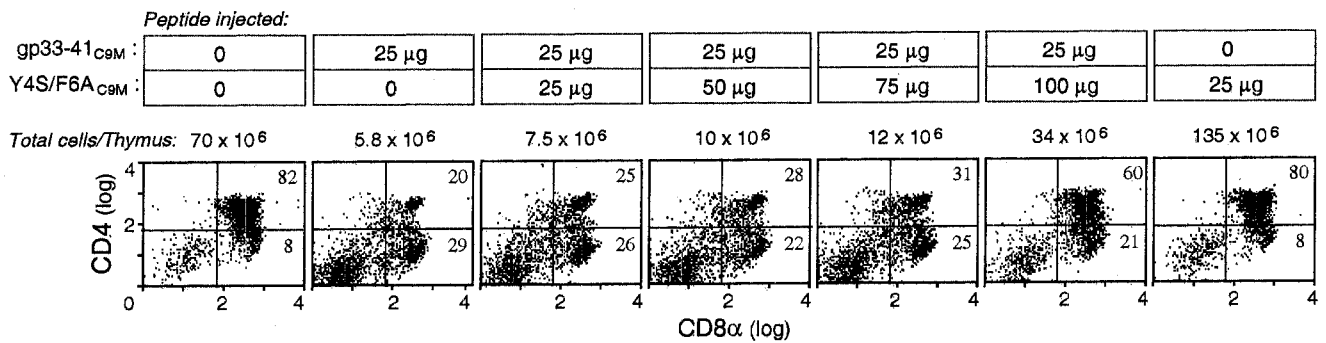


FIGURE 5. The Y4S/F6A_{C9M} variant peptide inhibits negative selection of thymocytes *in vivo*. P14 RAG2^{-/-} mice were injected three times with mixtures of gp33-41_{C9M} and Y4S/F6A_{C9M} variant at indicated concentrations. Eighteen hours after the third injection, thymocytes were double-stained with the CyChrome-anti-CD4 and FITC-anti-CD8α. The percentages of DP and SP CD8 subsets after gating on 50,000 live cells are indicated.

selecting peptides for binding to H-2D^b molecules expressed on thymic stroma either by binding to “empty” surface MHC class I molecules or, perhaps, by a cross-presentation mechanism (35).

Y4S/F6A peptide interacts with the P14 TCR with low affinity

To study the relative avidity of interactions between the P14 TCR and the gp33-41 variant peptides bound to H-2D^b molecules, we prepared tetramers of H-2D^b with each of the above peptides, and performed quantitative immunofluorescence analysis of thymocytes, splenocytes, and lymph node cells from P14 RAG2^{-/-} mice. The results of MFI staining of SP CD8 thymocytes from P14 RAG2^{-/-} mice with the three tetramers at different concentrations are depicted in Fig. 6. The *inset* shows representative staining profiles at a single comparable concentration of tetramer. Clearly, the strongest binding occurs with the tetramer containing the gp33-41_{C9M} peptide, as reflected by higher fluorescence intensity levels. Tetramer containing A7E_{C9M} mutant bound with lower affinity, whereas no detectable binding was observed with the tetramer refolded with the Y4S/F6A_{C9M} variant peptide. These results in conjunction with functional data (Fig. 1, B–D) suggest that the Y4S/F6A_{C9M} mutant must interact with the P14 TCR with extremely poor affinity, if at all.

Development of an *in vivo* model for thymocyte selection and emigration

To date, the processes of T cell development involving the interactions between the P14 TCR and the gp33-41 variant peptides have been studied exclusively in the transgenic mouse system. Although the homogeneity of TCR-expressing cells on the RAG2^{-/-} background is an advantage for specific analysis, it remains difficult to identify the numerically small population of recent thymic emigrants (RTE). To overcome this problem, we have used irradiation chimeras using congenic mouse strains (expressing the CD45.1 marker in B6 and CD45.2 in P14 and N15 transgenic mice). Previously, using N15 transgenic mice carrying a TCR specific for the VSV8 peptide in the context of H-2K^b, a weak agonist peptide variant L4, with the substitution of leucine for valine at the P4 peptide residue, inducing positive selection has been identified (16). We wondered whether interactions between the low affinity ligands, Y4S/F6A and L4, and their specific TCRs would result in thymic positive selection and emigration. Thus, lineage-negative BM precursors of P14 or N15 RAG2^{-/-} mice (donor) were injected into irradiated congenic B6 mice (recipient) and the development of donor-type cells was monitored weekly by immunofluorescence staining and multicolor FACS analysis. As shown in Fig. 7, donor-type P14-specific SP CD8 thymocytes appeared in the thymus 3–4 wk after BM injection, comprising

~70% of the SP CD8 subset by wk 5 (Fig. 7, *upper panel*). In contrast, almost no peripheral donor T cells have been detected in irradiation chimeras at 3–4 wk after BM injection (*middle and lower panels*, Fig. 7), although such cells are identifiable between 4 and 5 wk after injection. When BM cells from N15 RAG2^{-/-} mice were sorted and injected into irradiated B6 recipients, and the development of donor-type T cells was examined in an analogous manner, similar kinetics of maturation and emigration of N15 RAG2^{-/-}-specific SP CD8 T cells were found (data not shown). Therefore, we administered the selecting peptides to the recipient at 3–4 wk after donor BM injection and assessed whether such exposure might influence the subsequent selection and emigration processes of donor thymocytes.

Y4S/F6A and L4 variants of viral epitopes mediate positive selection and emigration of thymocytes

Between 3–4 wk post-BM reconstitution, gp33-41 and its variant peptides were injected daily for 3 days and animals examined 24 h

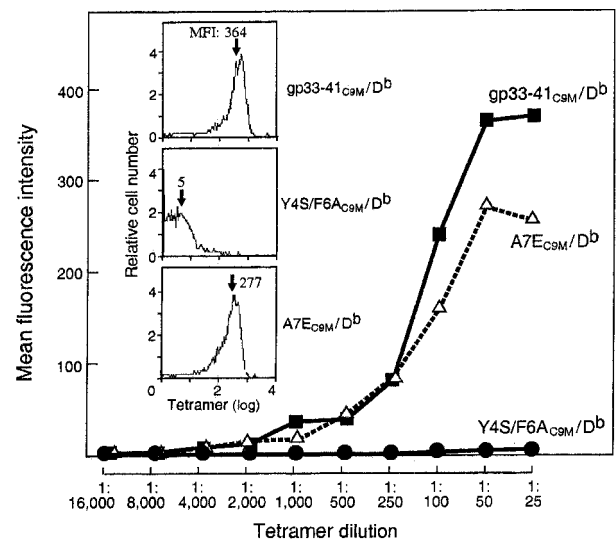


FIGURE 6. The Y4S/F6A_{C9M} variant peptide in complex with D^b does not bind to the P14 TCR with sufficient affinity to be measured by tetramer staining. Recombinant class I H-2D^b and β_{2m} proteins were refolded with each of the gp33-41_{C9M} variant peptides, biotinylated, and tetramerized using PE-avidin. Thymocytes from P14 RAG2^{-/-} mice at 4 wk of age were triple-stained with CyChrome-anti-CD4, FITC-anti-CD8α, and a PE-tetramer of one or another of the gp33-41 variant peptides at indicated dilutions. MFI of tetramer staining on gated SP CD8 thymocytes is shown. The *inset* shows histogram profiles of SP CD8 thymocyte staining with each of the tetramers at 1/50 dilution.

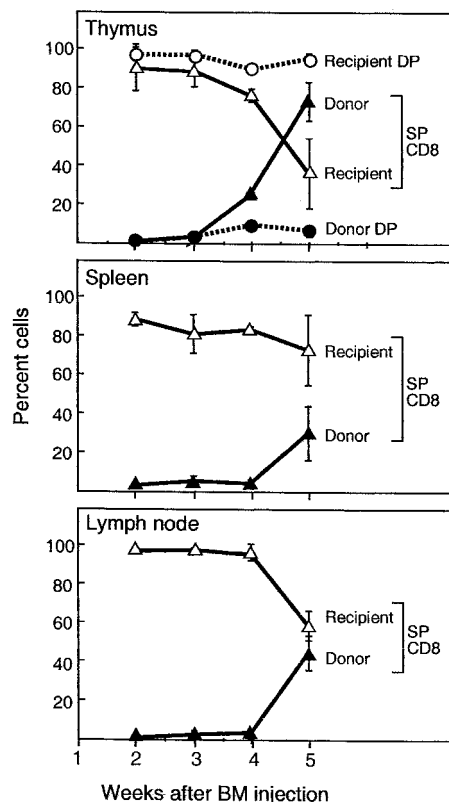


FIGURE 7. Kinetics of T cell development in irradiation chimeras of B6 Ly-5.1 mice reconstituted with BM from P14 RAG2^{-/-} (Ly-5.2) mice. B6 Ly-5.1 mice at 8 wk of age were injected with lineage-negative BM cells from P14 RAG2^{-/-} donors (1×10^6 cells per mouse) 2–4 h following irradiation (7 Gy). Thymuses, spleens, and lymph nodes were obtained weekly and cells were triple-stained with CyChrome-anti-CD4, PE-anti-CD8 α , and either FITC-anti-CD45.1 or FITC-anti-CD45.2. Results represent expression of donor (Ly-5.2) and recipient (Ly-5.1) phenotype on thymocytes, splenocytes, and lymph node cells. Mean \pm SD of two to four independent experiments is shown.

later. Fig. 8A, *upper four panels*, shows the anti-CD4 and anti-CD8 α profiles of all thymocytes in the recipient (both donor and host). Fig. 8A, *lower eight panels*, enumerate the donor (anti-CD45.2 reactive) cells in the DP and SP CD8 subpopulation as gated in the *upper panel*, with the absolute number of thymocytes given in the Fig. 8 *inset (right)*. The number of thymocytes in irradiation chimeras injected with Y4S/F6A_{C9M} was highest, whereas that of gp33–41_{C9M}-injected mice was lowest. This difference recapitulates the effect of gp33–41_{C9M} variant peptides vs gp33–41_{C9M} on thymocytes from P14 RAG2^{-/-} transgenic mice. Fig. 8A, *inset*, shows that the lowest DP numbers are in irradiation chimeras injected with gp33–41_{C9M} peptide, whereas DP numbers are increased in mice injected with the Y4S/F6A_{C9M} variant. The number of SP CD8 thymocytes was also highest in chimeras injected with Y4S/F6A_{C9M} variant peptide (Fig. 8A, *inset*), suggesting that this ligand mediated positive selection of P14 RAG2^{-/-}-specific T cells. As the increase in thymocyte numbers exceeds the donor-engrafted population, injection of Y4S/F6A_{C9M} peptide may lead to the rescue of certain nontransgenic thymocytes from negative selection as well.

To appreciate whether APL might function in an analogous manner in other systems to modulate selection, we have generated N15 RAG2^{-/-}-B6 irradiation chimeras, injected either VSV8, L4, or PBS and subjected the animals to comparable analysis. Here, as well, the number of thymocytes in irradiation chimeras injected with L4 was highest, whereas that of VSV8-injected mice was

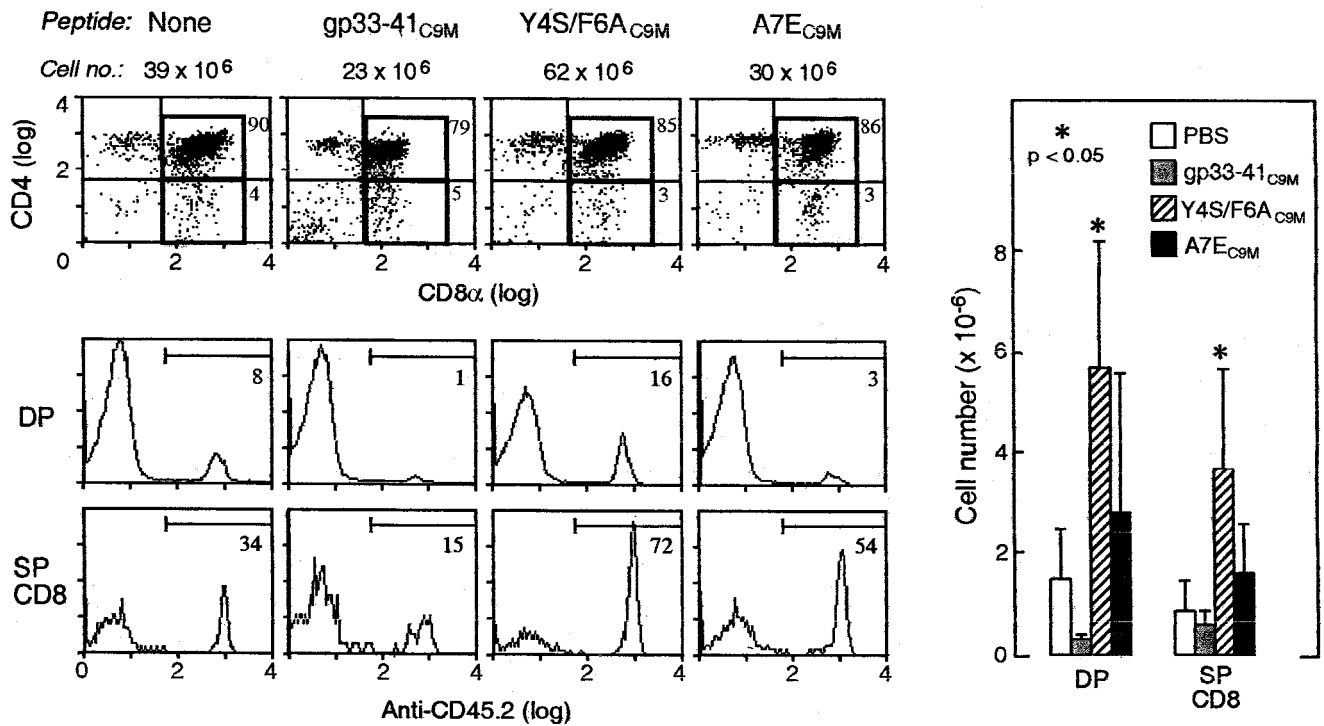
lowest (Fig. 8B, *inset*), similarly to the effect of gp33–41 variant peptides on thymocytes from P14 RAG2^{-/-}-B6 chimeras. The CD4/CD8 donor thymocyte profiles (Fig. 8B, *lower panel*) showed the lowest percentage of DP and SP CD8 thymocytes in irradiation chimeras injected with VSV8 peptide, compared with mice injected with L4 or with PBS. In contrast, the number of both DP and SP CD8 donor thymocytes was highest in chimeras injected with L4 variant peptide, consistent with positive selection.

To determine whether Y4S/F6A and L4 lead to emigration of SP CD8 thymocytes from the thymus to the periphery, spleens and lymph nodes from the same P14 RAG2^{-/-}-B6 and N15 RAG2^{-/-}-B6 irradiation chimeras analyzed in Fig. 8 were examined using triple-color immunofluorescence with anti-CD45.2, anti-CD8 α , and anti-V α 2 or -V β 5 mAbs. The results are represented in Fig. 9A, where the percentages of donor T cells in the host lymph nodes of P14 RAG2^{-/-}-B6 irradiation chimeras injected with gp33–41_{C9M} variant peptides are shown. Note that treatment with gp33–41_{C9M} leads to activation of the cognate P14 T cells, as judged by their size increase (Fig. 9A, *upper panel*) and down-regulation of the TCR (V α 2; Fig. 9A, *lower panel*), in line with previous observations in other TCR transgenic models (25). The greatest number of donor-type CD45.2⁺CD8⁺V α 2⁺ T cells (Fig. 9A, *inset*) was in the lymph nodes of Y4S/F6A_{C9M}-injected chimeras, suggesting that donor-type thymocytes developing in the presence of Y4S/F6A_{C9M} mature and emigrate to the lymph nodes. Similar increase in the numbers of donor-type cells in lymph nodes was observed 9 wk after injection of Y4S/F6A_{C9M} peptide (data not shown). The functional analysis of donor-type CD8⁺ lymph node T cells in irradiation chimeras injected with the positively selecting Y4S/F6A_{C9M} peptide showed \sim 2-fold higher proliferation levels in response to the cognate peptide gp33–41_{C9M} in vitro, compared with cells from PBS control-injected chimeric mice, reflecting the 2-fold difference in the number of donor-type CD8⁺ T cells in lymph nodes of chimeras injected with the Y4S/F6A_{C9M} peptide (data not shown). Note that Y4S/F6A_{C9M} peptide induces little emigration to spleen relative to the PBS control. In contrast, in N15 RAG2^{-/-}-B6 irradiation chimeras injected with the L4 variant, higher CD8⁺V β 5.2⁺ donor-type T cell numbers were observed both in lymph nodes and spleens, several days (Fig. 9B, *inset*) or 9 wk (data not shown) after L4 injection. The possible basis for this difference is described below, perhaps related to differential K^b vs D^b peptide presentation.

Mature donor-type T cells do not proliferate in response to Y4S/F6A or L4 variant peptides in vivo

To investigate the basis for the higher T cell numbers of the donor phenotype in the peripheral lymphoid tissues of mice injected with the Y4S/F6A or L4 peptides, we measured cell divisions in response to the above peptides in vivo. Sorted CD44⁻CD8⁺ splenocytes of P14 or N15 origin were labeled with CFSE before transfer into irradiated recipient congenic hosts. Four days later, the time interval allowing cells to settle in the peripheral organs, peptides were injected, and spleens and lymph nodes taken for FACS staining 3–4 days after the peptide injection. CFSE allowed assessment of the extent of proliferation of individual transferred T cells, as previously described (31). As shown in Fig. 10A, the percentage of CFSE⁺CD8⁺ cells was lowest in lymph nodes of irradiation chimeras injected with the gp33–41_{C9M} peptide, with no brightly CFSE⁺ cells remaining, suggesting that naive P14-specific T cells had undergone proliferation and activation-induced cell death (AICD) in response to the gp33–41_{C9M} ligand. In contrast, the percentage of CFSE⁺CD8⁺ T cells in mice injected with the Y4S/F6A_{C9M} peptide was similar to the control PBS-injected mice, implying that this peptide caused no T cell expansion. In chimeras

A



B

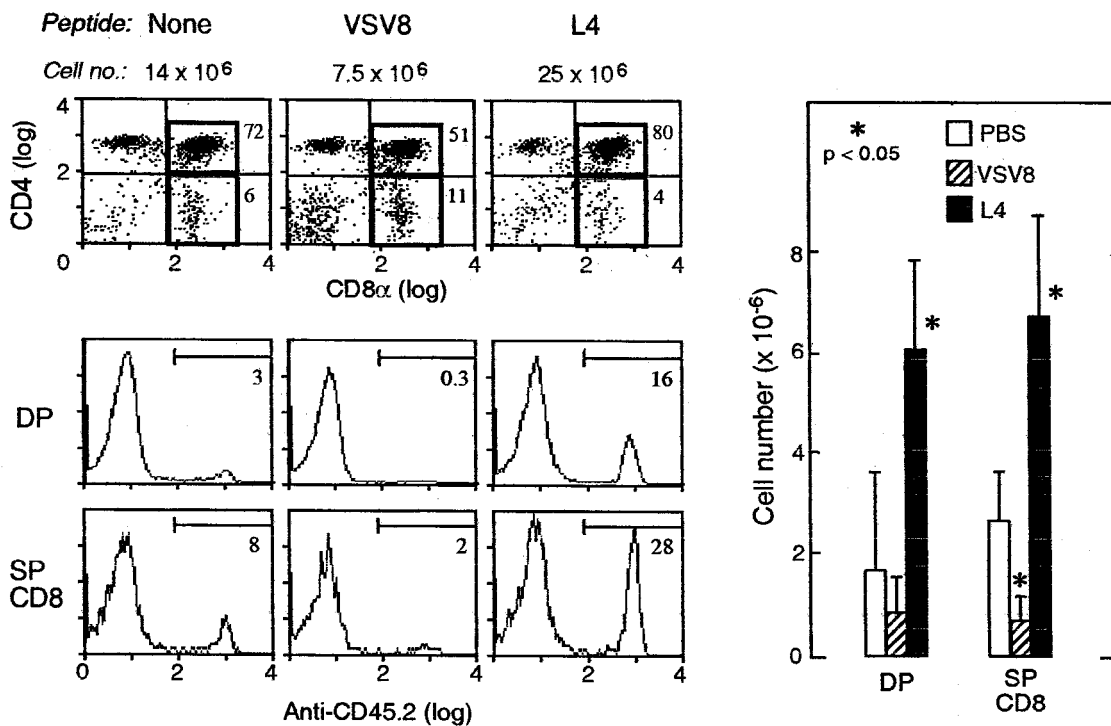


FIGURE 8. Y4S/F6A_{C9M} and L4 variants of viral epitopes mediate positive selection of thymocytes. Irradiated (7 Gy) B6 Ly-5.1 mice (8–10 wk of age) were injected i.v. with 25 μg of each peptide ≈4 wk after BM reconstitution. Thymocytes were triple-stained with CyChrome-anti-CD4, PE-anti-CD8α, and either FITC-anti-CD45.1 or FITC-anti-CD45.2. *A*, Upper panel, the CD4/CD8α profiles in thymuses reconstituted with P14 RAG2^{-/-}-derived BM progenitors as affected by gp33–41 (C9M) variant peptides. The percentages of DP and SP CD8 subsets after gating on 50,000 live cells are indicated. The histograms are of the donor phenotype (CD45.2) expression on the gated DP (middle panel), or SP CD8 (lower panel) thymocytes. The numbers represent the percentages of CD45.2-positive cells. The inset (right) shows absolute numbers of donor DP and SP CD8 subpopulations, based on the total thymocyte counts and the percentages of CD45.2-positive cells. Asterisks indicate *p* < 0.05 relative to PBS control according to Student's *t* test. Results represent mean ± SD of three independent experiments. *B*, The CD4/CD8α profiles (upper panel), histograms of the donor phenotype (CD45.2) expression on the gated DP (middle panel) and SP CD8 (lower panel) thymocytes in thymuses reconstituted with N15 RAG2^{-/-}-derived BM progenitors as affected by VSV8 and its variant L4 peptide. Other details as in *A*.

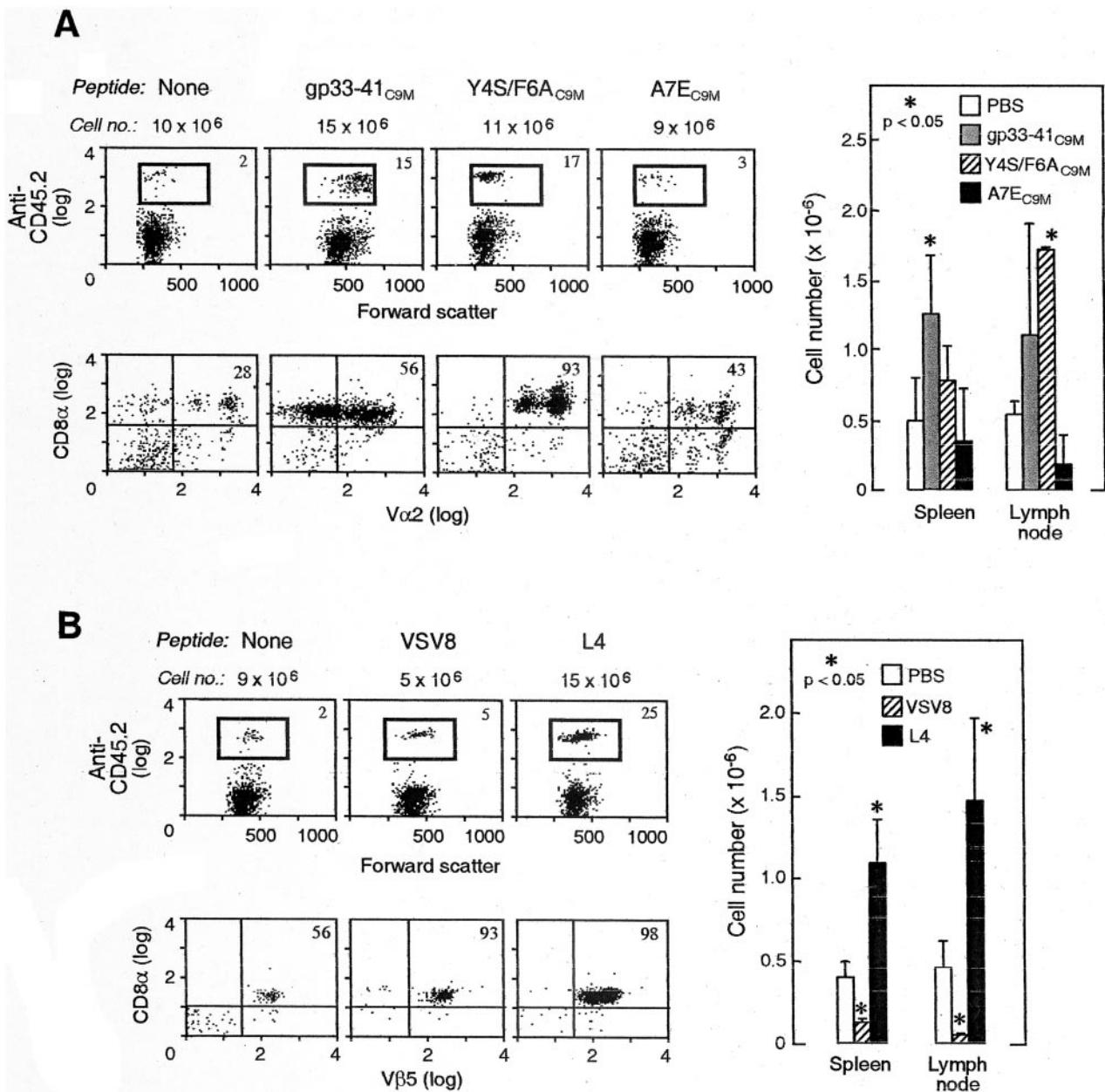


FIGURE 9. The Y4S/F6A_{C9M} variant leads to increased emigration of CD45.2⁺CD8⁺Vα2⁺ T cells to the lymph nodes of irradiation chimeras. Lymph node cells from Fig. 8 animals were triple-stained with CyChrome-anti-CD8α, PE-anti-Vα2, and either FITC-anti-CD45.1 or FITC-anti-CD45.2. *A*, *Upper panel*, the dot plot profiles of forward scatter/CD45.2 in lymph nodes of irradiation chimeras reconstituted with P14 RAG2^{-/-}-derived BM progenitors as affected by gp33-41_{C9M} variant peptides. The percentages of donor CD45.2⁺ T cells after gating on 25,000 live cells are indicated. *Lower panel*, The CD8α/Vα2 dot plot profiles of the gated CD45.2⁺ T cells. The numbers represent the percentages of CD8α⁺Vα2⁺-positive cells. *Inset*, Absolute numbers of donor CD45.2⁺ CD8α⁺Vα2⁺ splenocytes and lymph node cells, based on the total cell counts and the percentages of CD45.2-positive cells. Asterisks indicate $p < 0.05$ relative to PBS control according to the Student's *t* test. Results represent mean \pm SD of three independent experiments. *B*, The dot plot profiles of forward scatter/CD45.2 (*upper panel*), and the CD8α/Vβ5 dot plot profiles of the gated CD45.2⁺ T cells (*lower panel*) in lymph nodes of irradiation chimeras reconstituted with N15 RAG2^{-/-}-derived BM progenitors as affected by VSV8 and its variant L4 peptide. The numbers represent the percentages of CD45.2⁺CD8α⁺Vβ5⁺-positive cells. Other details as in *A*.

injected with the A7E_{C9M} peptide, the percentage of CFSE⁺CD8⁺ cells was higher than in gp33-41_{C9M}-injected mice, but lower than in Y4S/F6A_{C9M}-injected mice, consistent with the A7E_{C9M} variant inducing some degree of T cell proliferation. It must be noted that because the adoptive transfer is into irradiated recipients, donor-type cell proliferation is significant even in the absence of peptide administration (31, 36), based on the reduction in the intensity of CFSE staining of the control (PBS injected) chimeras (MFI = 121) as compared with the initial CFSE staining intensity of donor cells before injection (MFI = 9000).

CD44⁻CD8⁺ splenocytes from N15 RAG2^{-/-} mice were similarly labeled with CFSE and transferred into irradiated congenic hosts, followed by injection of VSV8 or L4 peptides (Fig. 10*B*). In the presence of VSV8, no brightly CFSE⁺CD8⁺ cells were detected in lymph nodes (Fig. 10*B*) or spleen (data not shown), suggesting that naive N15-specific T cells had undergone proliferation and AICD in response to the VSV8 ligand. In contrast, the number of CFSE⁺CD8⁺ T cells in mice injected with the L4 peptide was similar to the control group, implying that this peptide caused neither substantial T cell expansion or AICD. These data suggested

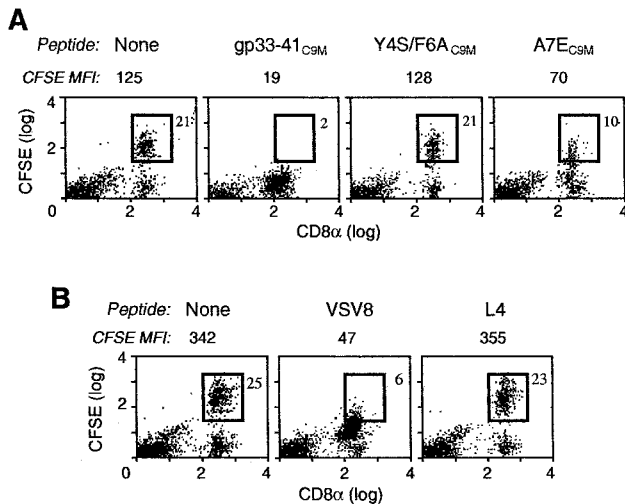


FIGURE 10. APL variants do not induce donor T cell divisions in the periphery of irradiated hosts. *A*, Sorted CD44⁻CD8⁺ CFSE-labeled P14 RAG2^{-/-} splenocytes (Ly-5.2; 2×10^6) were transferred to 7 Gy-irradiated B6 (Ly-5.1) mice. Four days later, gp33–41_{C9M} variant peptides were injected i.v. After an additional 4 days, spleen and lymph node cells were stained with CyChrome-anti-CD8 α . Numbers correspond to the percentages of CFSE⁺CD8 α ⁺ cells after gating on 25,000 live cells. Note that because the absolute number of splenocytes and lymph node cells is comparable in all groups, the percentage values are also representative of cell numbers. MFI of labeled cells before injection was 8300–9000. One of three representative independent experiments is shown. *B*, A total of 2×10^6 -sorted CD44⁻CD8⁺ CFSE-labeled N15 RAG2^{-/-} splenocytes (Ly-5.2) were transferred to 7 Gy-irradiated B6 (Ly-5.1) mice. Four days later, VSV8 and its variant L4 peptide were injected i.v. and subjected to a similar protocol as in *A*. One of two independent experiments is shown.

that cognate peptide ligands gp33–41 and VSV8, interacting with the TCR with relatively high affinity, compared with their respective APL, induce activation of peripheral T cells, whereas peptide variants Y4S/F6A and L4, which bind TCR with low affinity and mediate positive selection, do not cause cell divisions.

Discussion

Analysis of Y4S/F6A and A7E peptides in H-2^b mice represents the first examination of the direct effects of amino acid substitutions at the P14 TCR contact residues on thymocyte selection and activation in vivo. The crystal structure of gp33/H-2D^b suggests that single mutations at both peptide positions 4 (p4) or 6 (p6) directly affect TCR contacts (20, 21, 37). Those mutants of gp33–41 mediate positive selection presumably due to weaker pMHC/TCR interactions (19). In contrast to previous studies, in the present work mutations at p4 and p6 of gp33–41 were introduced in the same variant, to generate a positively selecting ligand with reduced TCR affinity to foster emigration of the developing thymocytes to the periphery. Indeed, Y4S/F6A_{C9M} was found to interact with the P14 TCR on SP CD8 thymocytes with an affinity below our detection limit, as judged by tetramer staining. In contrast to substitutions of amino acids at p4 plus p6, a single mutation at p7 did not significantly affect thymocyte subset numbers. However, the A7E_{C9M} variant altered the thymocyte phenotype (Fig. 2*B*). Our functional data (Fig. 1) suggest that A7E_{C9M} is a weak agonist of gp33–41. Consistent with the ability of peptides with the mutation at p7 to interact with the P14 TCR, incubation of P14 thymocytes with A7S in vitro in FTOC at high molarity resulted in negative selection (38).

Y4S/F6A_{C9M} induced up-regulation of the P14 TCR, the CD8 β coreceptor, and the β_7 integrin levels on SP CD8 thymocytes, characteristic of positive selection, with no change in the expres-

sion of other markers for activation/emigration/positive selection, including CD25, CD44, CD62L, and CD69. Characterization of RTE has been controversial. Up-regulation of several markers on SP CD8 thymocytes undergoing positive selection and emigration, including CD5 (39), β_7 integrin, CD44 and L-selectin (CD62L) has been reported (33, 40), whereas others did not observe these changes (41). Our data further demonstrate the heterogeneity of the phenotypes of SP CD8 thymocyte subpopulations affected by positively selecting ligands, as well as difficulties in the precise characterization of the small subpopulation of RTE. In contrast, gp33–41_{C9M} led to thymocyte activation and subsequent increase in the expression of CD44 and CD69, in line with similar observations in other models (25, 42, 43), whereas the A7E_{C9M} led to up-regulation of CD44, β_7 integrin and CD8 β (Fig. 2*B*).

The kinetics of reconstitution of irradiated hosts by thymocyte progenitors from the BM of P14- and N15-TCR transgenic mice was similar to the findings of Tanchot and Rocha (36). In addition, we show that thymocyte emigration is dependent on the affinity/avidity of pMHC/TCR interactions. Peripheral SP CD8 T cells of the donor phenotype, when transferred into the irradiated hosts later injected with Y4S/F6A_{C9M} or L4 ligands, did not expand, as judged by CFSE staining. “Background” proliferation did occur in a peptide-independent manner in chimeric hosts due to availability of niches caused by irradiation (31). These results suggest that although the low affinity pMHC/TCR interactions are insufficient to trigger cell divisions, differentiation nevertheless follows.

The nature and the number of APL involved in positive selection of MHC class I-restricted T cells and their relationship to antigenic peptides has been controversial (reviewed in Ref. 3 and references therein). Although most of the above studies have been performed in vitro, little is known about mechanisms of positive selection of CD8 T cells in vivo. Affinity measurements support the idea that positively selecting peptide ligand affinities are lower than those of negatively selecting ligands for TCRs, but additionally linked to their MHC binding/stability properties (44). A recent publication described an antagonist of H-2K^b-specific OT-I TCR and a variant of OVA 257–264 peptide, (E1), endogenously expressed by cortical epithelial cells of TAP-deficient mice, which mediated positive selection of CD8⁺ T cells in vivo (45). Our report supports the idea that weak pMHC class I/TCR interactions promote positive selection of SP CD8 thymocytes. Certainly the 10,000-fold weaker functional N15 T cell stimulation by L4 vs VSV8 peptide is consistent with the view (46). However, because Y4S/F6A_{C9M} in complex with H-2D^b has no detectable binding with the P14 TCR, we cannot exclude the possibility that this pMHC/TCR interaction is no greater than the basal level of P14 TCR binding to D^b in general. Two recent studies in class II MHC-restricted TCR transgenic mouse systems are also consistent with the notion that weak pMHC ligands may foster positive selection (47, 48).

Of importance is the observation that Y4S/F6A_{C9M} led to an increase in the number of DP thymocytes, a phenomenon which has not been reported to occur during positive selection. However, the binding of Y4S/F6A_{C9M} to D^b might possibly prevent other endogenous negatively selecting thymic peptides from binding and interacting with the TCR. Consistent with this possibility, we show that Y4S/F6A_{C9M} competes for binding to H-2D^b with the negatively selecting cognate peptide gp33–41 (Fig. 5).

Collectively, our data show that cognate peptides can be modified to create variants that result in selection, directly or indirectly, of desired TCR specificities at the level of thymic development. This exogenous peptide administration offers a potential of expanding repertoire generation in vivo in a manner useful to the organism. Whether these peptide-specific T cells generate stronger defense mechanisms

to fight viral infection or tumors in the normal, nontransgenic mouse, remains to be investigated. In this respect, exploring means of enhancing differentiation of thymocytes bearing desired TCRs, together with the understanding of the mechanism of thymocyte emigration to the periphery, would be of great importance. Several agents have been shown to inhibit thymic export (reviewed in Ref. 49), while a recent report described factors mediating emigration from the thymus (50). In the future, combined approach of exposing the subject to a positively selecting APL plus a thymic export-enhancing agent might generate a practical and efficient protective immunity.

Acknowledgments

We thank Dr. David Harrington (Department of Biostatistical Science, Dana-Farber Cancer Institute) for preparation and statistical analysis of Fig. 3A, and Dr. Diane Mathis and Dr. Linda Clayton for review of the manuscript.

References

- Miller, J. F. 2002. The discovery of thymus function and of thymus-derived lymphocytes. *Immunol. Rev.* 185:7.
- Robey, E., and B. J. Fowlkes. 1994. Selective events in T cell development. *Annu. Rev. Immunol.* 12:675.
- Starr, T. K., S. C. Jameson, and K. A. Hogquist. 2003. Positive and negative selection of T cells. *Annu. Rev. Immunol.* 21:139.
- Goldrath, A. W., and M. J. Bevan. 1999. Selecting and maintaining a diverse T-cell repertoire. *Nature* 402:255.
- Garcia, K. C., L. Teyton, and I. A. Wilson. 1999. Structural basis of T cell recognition. *Annu. Rev. Immunol.* 17:369.
- Wang, J.-H., and E. Reinherz. 2001. Structural basis of T cell recognition of peptides bound to MHC molecules. *Mol. Immunol.* 38:1039.
- Stern, L. J., and D. C. Wiley. 1994. Antigenic peptide binding by class I and class II histocompatibility proteins. *Structure* 2:245.
- Hennecke, J., and D. C. Wiley. 2002. Structure of a complex of the human $\alpha\beta$ T cell receptor (TCR) HA1.7, influenza hemagglutinin peptide, and major histocompatibility complex class II molecule, HLA-DR4 (DRA*0101 and DRB1*0401): insight into TCR cross-restriction and allelic activity. *J. Exp. Med.* 195:571.
- Reche, P. A., and E. L. Reinherz. 2003. Sequence variability analysis of human class I and class II MHC molecules: functional and structural correlates of amino acid polymorphisms. *J. Mol. Biol.* 331:623.
- Evavold, B. D., J. Sloan-Lancaster, and P. M. Allen. 1993. Tickling the TCR: selective T cell functions stimulated by altered peptide ligands. *Immunol. Today* 14:602.
- De Magistris, M. T., J. Alexander, M. Coggeshall, A. Altman, F. C. A. Gaeta, H. M. Grey, and A. Sette. 1992. Antigen analog-major histocompatibility complexes act as antagonists of the T cell receptor. *Cell* 68:625.
- Hogquist, K. A., S. C. Jameson, W. R. Heath, J. L. Howard, M. J. Bevan, and F. R. Carbone. 1994. T cell receptor antagonist peptides induce positive selection. *Cell* 76:17.
- Ashton-Rickardt, P. G., A. Bandeira, J. R. Delaney, L. Van Kaer, H. P. Pircher, R. M. Zinkernagel, and S. Tonegawa. 1994. Evidence for a differential avidity model of T cell selection in the thymus. *Cell* 76:651.
- Page, D. M., J. Alexander, K. Snoko, E. Apella, A. Sette, S. M. Hedrick, and H. M. Grey. 1994. Negative selection of CD4⁺CD8⁺ thymocytes by T-cell receptor peptide antagonists. *Proc. Natl. Acad. Sci. USA* 91:4057.
- Spain, L. M., J. L. Jorgensen, M. M. Davis, and L. J. Berg. 1994. A peptide Ag antagonist prevents the differentiation of T cell receptor transgenic thymocytes. *J. Immunol.* 152:1709.
- Ghendler, Y., M.-K. Teng, J.-H. Liu, T. Witte, J. Liu, K. S. Kim, P. Kern, H.-C. Chang, J.-H. Wang, and E. L. Reinherz. 1998. Differential thymic selection outcomes stimulated by focal structural alteration in peptide/major histocompatibility complex ligands. *Proc. Natl. Acad. Sci. USA* 95:10061.
- Pircher, H. P., R. Burki, R. Lang, H. Hengartner, and R. M. Zinkernagel. 1989. Tolerance induction in double-specific T cell receptor transgenic mice varies with antigen. *Nature* 342:559.
- Puglielli, M. T., A. J. Zajac, R. G. van der Most, J. L. Dzurik, A. Sette, J. D. Altman, and R. Ahmed. 2001. In vivo selection of a lymphocytic choriomeningitis virus variant that affects recognition of the gp33-41 epitope by H^b but not H-2K^b. *J. Virol.* 75:5099.
- Nguyen, L. T., M. F. Bachmann, and P. S. Ohashi. 2002. Contribution of LCMV transgenic models to understanding T lymphocyte development, activation, tolerance, and autoimmunity. *Curr. Top. Microbiol. Immunol.* 263:119.
- Tissot, A. C., C. Ciatto, P. R. Mittl, M. G. Grutter, and A. Pluckthun. 2000. Viral escape at the molecular level explained by quantitative T-cell receptor/peptide/MHC interactions and the crystal structure of a peptide/MHC complex. *J. Mol. Biol.* 302:873.
- Achour, A., J. Michaelsson, R. A. Harris, J. Odeberg, P. Grufman, J. K. Sandberg, V. Levitsky, K. Karre, T. Sandalova, and G. Schneider. 2002. A structural basis for LCMV immune invasion: subversion of H-2D^b and H-2K^b presentation of gp33 revealed by comparative crystal structure analyses. *Immunity* 17:757.
- Townsend, A. R., A. J. McMichael, N. P. Carter, J. A. Huddlestone, and G. G. Brownlee. 1984. Cytotoxic T cell recognition of the influenza nucleoprotein and hemagglutinin expressed in transfected mouse L cells. *Cell* 39:13.
- Williams, O., R. Tarazona, A. Wack, N. Harker, K. Roderick, and D. Kioussis. 1998. Interactions with multiple peptide ligands determine the fate of developing thymocytes. *Proc. Natl. Acad. Sci. USA* 95:5706.
- Smyth, L. A., O. Williams, R. D. Huby, T. Norton, O. Acuto, S. C. Ley, and D. Kioussis. 1998. Altered peptide ligands induce quantitatively but not qualitatively different intracellular signals in primary thymocytes. *Proc. Natl. Acad. Sci. USA* 95:8193.
- Mamalaki, C., T. Norton, Y. Tanaka, A. R. Townsend, P. Chandler, E. Simpson, and D. Kioussis. 1992. Thymic depletion and peripheral activation of class I major histocompatibility complex-restricted T cells by soluble peptide in T-cell receptor transgenic mice. *Proc. Natl. Acad. Sci. USA* 89:11342.
- Ghendler, Y., R. E. Hussey, T. Witte, E. Mizoguchi, L. K. Clayton, A. K. Bhan, S. Koyasu, H. C. Chang, and E. L. Reinherz. 1997. Double positive T cell receptor high thymocytes are resistant to peptide/major histocompatibility complex ligand-induced negative selection. *Eur. J. Immunol.* 27:2279.
- Shibata, K.-I., M. Imarai, G. M. van Bleek, S. Joyce, and S. G. Nathanson. 1992. Vesicular stomatitis virus antigenic octapeptide N52-59 is anchored into the groove of the H-2K^b molecule by the side chains of three amino acids and the main-chain atoms of the amino terminus. *Proc. Natl. Acad. Sci. USA* 89:3135.
- Moody, A. M., Y. Xiong, H. C. Chang, and E. L. Reinherz. 2001. The CD8 $\alpha\beta$ co-receptor on double-positive thymocytes binds with differing affinities to the products of distinct class I MHC loci. *Eur. J. Immunol.* 31:2791.
- Sasada, T., Y. Ghendler, J. M. Neveu, W. S. Lane, and E. L. Reinherz. 2001. A naturally processed mitochondrial self-peptide in complex with thymic MHC molecules functions as a selecting ligand for a viral-specific T cell receptor. *J. Exp. Med.* 194:883.
- Sasada, T., M. Touma, H.-C. Chang, L. K. Clayton, J.-H. Wang, and E. L. Reinherz. 2002. Involvement of the TCR C β FG loop in thymic selection and T cell function. *J. Exp. Med.* 195:1419.
- Bender, J., T. Mitchell, J. Kappler, and P. Marrack. 1999. CD4⁺ T cell division in irradiated mice requires peptides distinct from those responsible for thymic selection. *J. Exp. Med.* 190:367.
- Wang, B., A. Sharma, R. Maile, M. Saad, E. J. Collins, and J. A. Frelinger. 2002. Peptidic termini play a significant role in TCR recognition. *J. Immunol.* 169:3137.
- Gabor, M. J., D. I. Godfrey, and R. Scollay. 1997. Recent thymic emigrants are distinct from most medullary thymocytes. *Eur. J. Immunol.* 27:2010.
- Tarazona, R., O. Williams, D. Moskophidis, L. A. Smyth, Y. Tanaka, M. Murdjeva, A. Wack, C. Mamalaki, and D. Kioussis. 1998. Susceptibility and resistance to antigen-induced apoptosis in the thymus of transgenic mice. *J. Immunol.* 160:5397.
- Ackerman, A. L., C. Kyritsis, R. Tampe, and P. Cresswell. 2003. Early phagosomes in dendritic cells form a cellular compartment sufficient for cross presentation of exogenous antigens. *Proc. Natl. Acad. Sci. USA* 100:12889.
- Tanchot, C., and B. Rocha. 1997. Peripheral selection of T cell repertoires: the role of continuous thymus output. *J. Exp. Med.* 186:1099.
- Young, A. C., W. Zhang, J. C. Sacchettini, and S. G. Nathanson. 1994. The three-dimensional structure of H-2D^b at 2.4 Å resolution: implications for antigen-determinant selection. *Cell* 76:39.
- Mariathasan, S., M. F. Bachmann, D. Bouchard, T. Ohteki, and P. S. Ohashi. 1998. Degree of TCR internalization and Ca²⁺ flux correlates with thymocyte selection. *J. Immunol.* 161:6030.
- Azzam, H. S., A. Grinberg, K. Liu, H. Shen, E. W. Shores, and P. E. Love. 1998. CD5 expression is developmentally regulated by T cell receptor (TCR) signals and TCR avidity. *J. Exp. Med.* 188:2301.
- Almeida, A., A. M. Borghans, and A. A. Freitas. 2001. T cell homeostasis: thymus regeneration and peripheral T cell restoration in mice with a reduced fraction of competent precursors. *J. Exp. Med.* 194:591.
- Lee, C. K., K. S. Kim, L. A. Welniak, W. J. Murphy, K. Muegge, and S. K. Durum. 2001. Thymic emigrants isolated by a new method possess unique phenotypic and functional properties. *Blood* 97:1360.
- Murphy, N. M., A. B. Heimberger, and D. Y. Loh. 1990. T cell deletion follows chronic antigen specific T cell activation in vivo. *Science* 250:1720.
- Liblau, R. S., R. Tisch, K. Schokat, X.-D. Yang, N. Dumont, C. Goodnow, and H. O. McDevitt. 1996. Intravenous injection of soluble antigen induces thymic and peripheral T cell apoptosis. *Proc. Natl. Acad. Sci. USA* 93:3031.
- Holmberg, K., S. Mariathasan, T. Ohteki, P. S. Ohashi, and N. R. Gascoigne. 2003. TCR binding kinetics measured with MHC class I tetramers reveal a positive selecting peptide with relatively high affinity for TCR. *J. Immunol.* 171:2427.
- Stefanski, H. E., D. Mayerova, S. C. Jameson, and K. A. Hogquist. 2001. A low affinity TCR ligand restores positive selection of CD8⁺ T cells in vivo. *J. Immunol.* 166:6602.
- Sasada, T., Y. Ghendler, J. H. Wang, and E. L. Reinherz. 2000. Thymic selection is influenced by subtle structural variation involving the p4 residue of an MHC class I-bound peptide. *Eur. J. Immunol.* 30:1281.
- Kraj, P., R. Pacholczyk, H. Igantowicz, P. Kisielow, P. Jensen, and L. Ignatowicz. 2001. Positive selection of CD4⁺ T cells is induced in vivo by agonist and inhibited by antagonist peptides. *J. Exp. Med.* 194:407.
- Williams, C. D., D. L. Engle, G. J. Kersh, J. Michael White, and P. M. Allen. 1999. A kinetic threshold between negative and positive selection based on the longevity of the T cell receptor-ligand complex. *J. Exp. Med.* 189:1531.
- Rosen, H., G. Sanna, and C. Alfonso. 2003. Egress: a receptor-regulated step in lymphocyte trafficking. *Immunol. Rev.* 195:160.
- Poznansky, M. C., I. T. Olszak, R. H. Evans, Z. Wang, R. B. Foxall, D. P. Olson, K. Weibrecht, A. D. Luster, and D. T. Scadden. 2002. Thymocyte emigration is mediated by active movement away from stroma-derived factors. *J. Clin. Invest.* 109:1101.